



Electrospun Poly (Vinyl Alcohol) Nanofibrous Mat Loaded with Green Propolis Extract, Chitosan and Nystatin as an Innovative Wound Dressing Material

Maria S. Morais¹ · Daniela P. F. Bonfim² · Mônica L. Aguiar² · Wanderley P. Oliveira¹

Accepted: 23 August 2022

© The Author(s), under exclusive licence to Springer Science+Business Media, LLC, part of Springer Nature 2022

Abstract

Purposes The objective of this work was to produce and characterise biodegradable poly (vinyl alcohol) (PVA) nanofibre loaded with green propolis extract (GPE), chitosan (CS) and nystatin (NYS) alone and in mixtures as a potential wound dressing material.

Methods The GPE, NYS and CS1% were loaded in electrospinning compositions based on PVA 7%, 8% and 12% solubilised in milli-Q water or a mixture of water and glacial acetic acid. The electrospinning compositions without actives (blank) and those loaded with actives were characterised by determining the pH, electrical conductivity and rheological properties. An image analysis procedure applied to photomicrographs obtained by scanning electronic microscopy (SEM) allowed the determination of the nanofibres' diameter distribution and average surface porosity. The disintegration time and swelling ratio of the nanofibre mats were also determined.

Results The physicochemical parameters of the electrospinning compositions (pH, electrical conductivity and rheology) and the incorporated active ingredients (GPE, CS and NYS) affected the electrospun nanofibre mats properties. The electrospun nanofibres' mean diameters and surface porosity ranged from 151.5 to 684.5 nm and from 0.29 ± 0.04 to 0.50 ± 0.05 . The PVA/CS electrospun nanofibres fibres exhibited the smallest diameters, high surface porosity, water absorption capacity and disintegration time. The characteristics of the PVA/CS nanofibres mat associated with the biodegradability of the polymers make them a novel material with the potential to be applied as wound and burn dressings.

Keywords Nanofibres electrospinning · Image analysis · Propolis · Antimicrobial · Smart wound dressing

Introduction

The need for efficient and accurate solutions in various industrial sectors has stimulated the development of novel materials and processes to obtain them. Special attention is given to the biomaterials used in a wide range of devices for human health, such as vascular stents, dental restorations, artificial hips and contact lenses [1, 2]. Among the widely studied biomaterials, nanofibres have a prominent place. Nanofibres

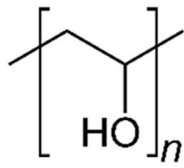
are nanostructures in the form of a mat of very thin and tangled fibres. They have applications in several knowledge fields due to their inherent properties, such as a high surface area, microporous structure, excellent stability and easy functionality. Nanofibres have been used as a drug delivery system [3, 4], scaffolding [5] and as dressings for wounds and burns [6].

Various methods can be used to produce nanofibres, and among them, electrospinning is a promising and efficient technique. Electrospinning uses electrostatic forces to elongate fine fibres from a polymeric composition, forming a fibre mat [7, 8]. The selection of the polymeric material (pure or mixed) used in the preparation of the formulations as well as its concentration and physicochemical properties are extremely important factors in the success of the operation and for obtaining electrospun fibres with properties suitable for the desired application (for example, wound dressing and drug delivery, among others). Natural (e.g. chitosan, pullulan, gelatin and collagen) and synthetic polymers (e.g. polylactic

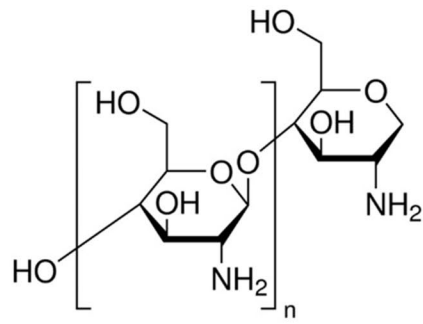
✉ Wanderley P. Oliveira
wpoliv@fcfrp.usp.br

¹ Laboratory of Pharmaceutical Processes, LAPROFAR, Faculty of Pharmaceutical Sciences of Ribeirão Preto, University of São Paulo, Ribeirão Preto 14040-903, Brazil

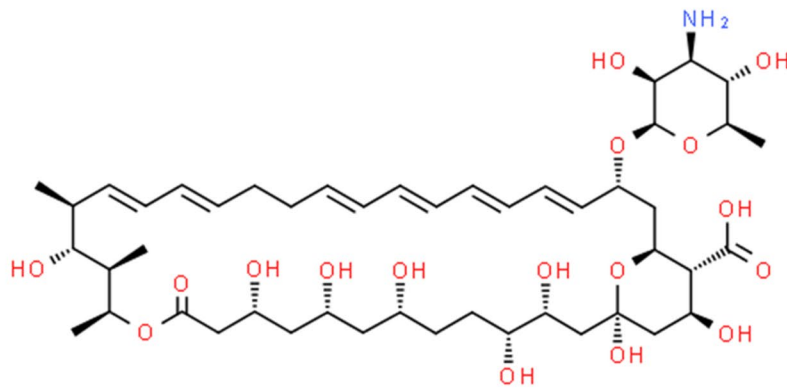
² Department of Chemical Engineering, University Federal of São Carlos, Rod. Washington Luiz, km 235, São Carlos, SP, Brazil



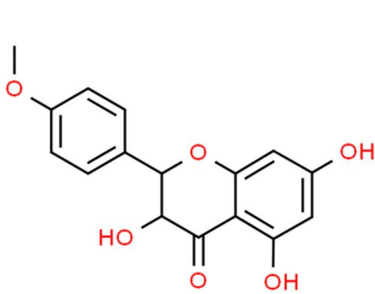
Poly(vinyl) alcohol



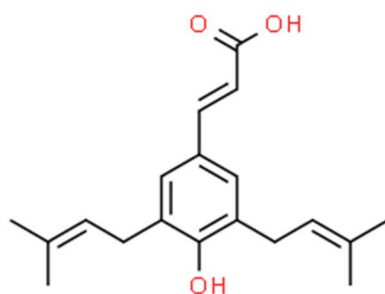
Chitosan



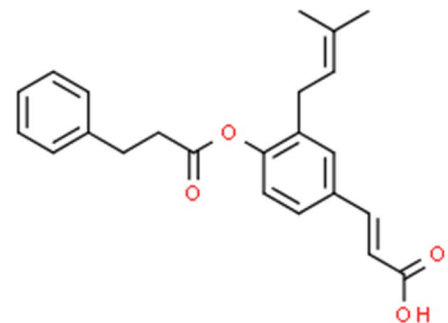
Nystatin



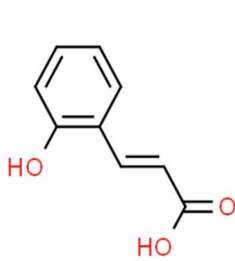
aromadendrin-4'-methyl ether



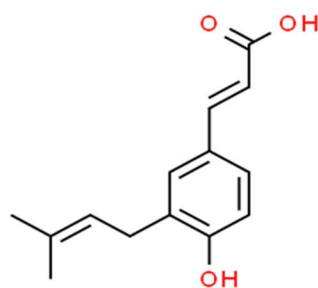
Artepellin C



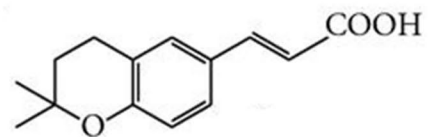
Baccharin



Coumaric acid



Drupanin



2,2-dimethyl-6-carboxyethenyl-2H-1-benzopyran

◀**Fig. 1** Molecular weight, chemical formula and structure of the PVA, chitosan, nystatin* and of selected constituents of the green propolis extract used*, namely coumaric acid, artepelin C, baccharin, drupanin, aromadendrin-4'-methyl ether and 2,2-dimethyl-6-carb-oxymethyl-2H-1-benzopyran (DCBEN) [27]. * Source: <https://pubchem.ncbi.nlm.nih.gov/>

acid – PLA, polymethacrylate – PMMA and polyethylene oxide – PEO) – alone or in blends – are commonly used for nanofibre production [9]. PVA is a semi-crystalline, synthetic organic polymer that is biodegradable under aerobic and anaerobic conditions. It has been widely used to prepare biomaterials such as hydrogels, films, membranes, scaffolds and nanofibres [10, 11]. Pharmaceutical uses of PVA include topical and ophthalmic formulations, stabilising agents for emulsions, and sustained release formulations for oral use. It is biocompatible, water-soluble, easy to process and has good chemical and thermal stability [10, 12]. These properties make the PVA an ideal material for the production of electrospun nanofibres loaded with active pharmaceutical ingredients; for example, herbal extracts (e.g. *Ziziphus jujube* Mill. [13], *Aloe vera* [14] and *Glycyrrhiza glabra* [15]), non-steroidal anti-inflammatory drug (sodium salicylate, diclofenac sodium, indomethacin and naproxen) for transdermal drug delivery, and to improve the solubility of the poorly water-soluble drug Probucol [16].

The electrospinning process is influenced by the physical and chemical properties of the electrospinning composition such as pH, electrical conductivity, rheological properties, solvent system and the type and concentration of polymeric material. The equipment's operating conditions – electrical potential, the distance between the collector and the feeding needle, the diameter of the feeding needle and the feed flow rate of the electrospinning composition – and the environmental conditions of temperature and relative humidity affect the process and properties of the fibre mats formed. They should be optimised prior to use [17–20]. The use of volatile solvents in the preparation of the composition is preferable as they favour removal during electrospinning.

An overview of the current literature indicates several studies that have evaluated the influence of processing conditions on the properties of the nanofibres formed [21–23]. However, given the process complexity and the lack of robust theoretical analysis, experimental studies are needed for each polymeric composition processed and equipment configuration.

This work aimed to evaluate the feasibility of electrospinning to produce biodegradable nanofibres from polyvinyl alcohol (PVA) loaded with active pharmaceutical ingredients (APIs), directed at future pharmaceutical applications (e.g. as biodegradable dressings for wounds and burns). Three different APIs with proven antimicrobial efficacy were selected to be incorporated into nanofibres (pure or in blends): green propolis extract [24], chitosan [12,

25] and nystatin [26]. Figure 1 shows the chemical structures of the PVA, chitosan, nystatin and of selected constituents of the green propolis extract used, namely coumaric acid, artepelin C, baccharin, drupanin, aromadendrin-4'-methyl ether and 2,2-dimethyl-6-carb-oxymethyl-2H-1-benzopyran (DCBEN) [27]. The resulting polymeric solutions with and without APIs were characterised by determining the pH, electrical conductivity and rheological behaviour. Electrospun nanofibres were successfully engineered and characterised by morphology, fibre diameter distribution and average surface porosity. The disintegration time and swelling capacity in the aqueous environment were also evaluated.

Materials and Methods

Materials

Polyvinyl alcohol (PVA), with a molecular weight of 85,500 g/mol and a degree of hydrolysis of 89.5% (Vetec Química Fina, Duque de Caxias – RJ, Brazil), chitosan (CS) (Polymar Ind. Com. Imp. and Exp. LTDA), deacetylation degree of 68.5% [28], glacial acetic acid (G) at 99.0% (LabSynth, Diadema – SP, Brazil) and Nystatin A1 trihydrate (NYS – CAS 34786–70-4 – Fagron Farmacêutica LTD, São Paulo – SP, Brazil) were the chemicals used. Southeastern Brazilian *Baccharis dracunculifolia* DC. green propolis (from Cajuru – SP, Brazil) was kindly provided by Professor Jairo Kenupp Bastos (University of São Paulo, Brazil). The complete chemical characterisation of the green propolis used was reported by de Sousa et al. [27]. Other reagents used were ethanol and methanol (analytical degree – LabSynth, Diadema – SP, Brazil), caffeic, cinnamic and ferulic acids (HPLC standards – Sigma Aldrich, Darmstadt, Germany), solvents HPLC grade (Sigma Aldrich, Darmstadt, Germany) and Milli-Q water (Millipore, Bedford, USA).

Electrospinning Apparatus

The electrospinning apparatus was constituted by a high voltage (0 to 50 kV) direct current source (Electrotest HIPOT CC, Model EH6005C), an infusion pump (Harvard, Model Elite I/W PROGR SINGLE) and a nanofibre collector consisting of a stainless-steel cylinder with a diameter of 100 mm and length of 200 mm. The nanofibre collector was coupled to a variable speed motor that allowed for changing the collector's rotation speed up to 600 rpm. The electrospinning process took place inside a fully grounded, electrically insulated compartment to minimise the occurrence of electrical discharges during operation.

Experimental Methods

Preparation of the Concentrated Green Propolis Extract

First, the crude green propolis (kept under refrigeration at 8 °C for 12 h) was grounded to a fine powder using a laboratory blender. The particle size was standardised by sieving in a 42-mesh sieve. Hence, 80 g of the powdered propolis was placed in contact with 1200 mL of a hydroethanolic solution at 70% (v/v) in a jacketed stirred vessel (dynamic maceration) at a controlled temperature of 50 °C [29] for 180 min. The extract was filtered and concentrated three times in a rotary evaporator to remove the excess ethanol. After cooling, the concentrated extract was centrifuged at 1056 g-force for 10 min in an Eppendorf centrifuge (5430 R) to remove the non-soluble material. The supernatant (green propolis extract (GPE)) was withdrawn and used as the GPE active ingredient in the nanofibres production. The solid concentration of the GPE was 5.5% (w/w) determined in a moisture analyser balance Sartorius MA-35 (Sartorius Lab Instruments GmbH & Co. KG, Goettingen, DE).

Chemical Characterisation of the Concentrated Green Propolis Extract

High-performance liquid chromatography with diode array detection (HPLC–DAD) is a method widely used for the separation, quantification and characterisation of the constituents of complex samples such as the GPE and herbal extracts [29–31]. Hence, a qualitative chemical characterisation of the GPE was done by obtaining its HPLC–DAD chromatographic profile (fingerprint) according to the method described by de Sousa et al. [27]. Analyses were performed in an HPLC Shimadzu Prominence LC-20A series using an LC-6A double pump (Shimadzu Corporation, Kyoto, Japan) using a C-18 column (Shimadzu Shim – Pack CLC(M) 4.6 mm × 25 cm, a particle diameter of 5 μm, a pore diameter of 100 Å) at 30 °C. The gradient analysis started with the mixture consisting of 75% of solvent A (acetic acid/ammonium acetate/methanol/water at the ratio of 0.8:0.3:5.0:93.9 v/w) and 25% of solvent B (acetonitrile), increasing linearly up to 100% of B over 60 min at a flow rate of 1.0 mL/min. The diode array detector (DAD) monitored the spectral data over the HPLC run at 270 to 320 nm. The chromatographic profiles were plotted at 280 nm. The sample of the GPE was diluted in methanol at a concentration of 5 mg/mL and filtered through a 0.45 μm Millipore membrane, while 10 μL was injected into the chromatograph. Standard methanolic solutions of caffeic acid (50 μg/mL), cinnamic acid (25 μg/mL) and ferulic acid (50 μg/mL) were prepared, and 10 μL was also injected into the chromatograph. Confirmation of the quality and authenticity of the GPE was performed by comparing the HPLC fingerprint, retention times and UV

spectra of the GPE with the previous results reported in the literature [27].

Preparation of the PVA Solutions Loaded with GPE, NYS and CS

The polymer concentrations used were chosen based on preliminary electrospinning runs, processing issues and data reported in the literature [32–34]. At concentrations of PVA and chitosan higher than 12% and 3%, the composition viscosity increases significantly, turning the electrospinning very hard to conduct. On the other hand, the composition rheology and solid concentration at small concentrations can hinder the electrospinning or increase the processing time needed to produce an adequate nanofibre mat (data not shown). The selected ranges allowed obtaining electrospun nanofibre mats of high quality. Hence, PVA solutions at 7% and 8% w/v (PVA/W7% and PVA/W8%) were prepared by mixing weighed amounts of PVA in purified water at a temperature between 80 and 90 °C, maintaining the mixtures under stirring until complete dissolution. After cooling, the crude extract of green propolis was incorporated into the PVA 7% solution at 70:30 w/w (F1). The formulation loaded with GPE and Nystatin was obtained by adding the GPE in the PVA/W8% solution, then 20 mg of nystatin, solubilised previously in 1 ml of methanol. The resulting proportion used was 70:30:20 mg (PVA: GPE: NYS – formulation F2). Stirring was maintained until complete incorporation (~60 min). The same procedure was used to prepare the PVA solution at 12% (w/v). However, the solvent system was a water:glacial acetic acid solution at a 70:30 ratio (PVA/G12%). Chitosan acetate solution at 1% (w/v) was prepared by mixing a weighed amount of powdered chitosan in water:glacial acetic acid (30:70) at room temperature, maintained under stirring for 60 min (CS1%). The CS electrospinning solutions were prepared by blending the formulations PVA/G12% and CS1% at the proportion of 50:50 (F3). Additionally, 20 mg of NYS was weighed and solubilised in 1 ml of methanol and mixed with PVA/G12%. The mixture was kept under stirring for 60 min for the complete incorporation (formulation F4). Finally, PVA/G12% + CS1% + NYS was prepared at a ratio of 50:50:20 mg (F5). The volume total of the formulations prepared was 50 mL, independent of their compositions.

The five different compositions tested were set to demonstrate the potential of the PVA alone or blended with CS for the production of versatile electrospun nanofibres loaded with antimicrobial agents GPE and NYS and were based on the literature reports and preliminary assays [35–37]. The antimicrobial properties of GPE and NYS are well described in the literature, besides the use in the practical clinic (NYS).

Potential of the Hydrogen (pH), Electrical Conductivity and Rheology of the Formulations

The properties of electrospun nanofibre mats formed are significantly affected by the physicochemical properties of the electrospinning formulations (e.g. hydrogen potential – pH, electrical conductivity and rheological behaviour) [14]. These properties were determined for formulations F1 to F5 and blank formulations (without the addition of actives), namely PVA/W7% and PVA/W8%, PVA/G12% and CS1%.

The pH of formulations F1 to F5 was determined in a previously calibrated digital pH metre Metrohm, model 827 (Metrohm AG, Herisau – CH), while the electrical conductivities were measured at room temperature in a Metrohm 912 bench-top conductometer (Metrohm AG, Herisau, Switzerland). The measurements were done in triplicate, and the results were expressed as means and standard deviation.

The rheology of formulations F1 to F5 and blank solutions was determined with a Brookfield LV-DVIII coaxial cylinder Rheometer (Brookfield Engineering Laboratories Inc., Middleboro, USA), equipped with the small sample adapter and SC4-18 spindle sensor. The formulation was placed into the small sample adapter, and the spindle was coupled to the equipment. After calibrating the system, the spindle rotation started, and the velocities were increased according to the preset programme. After reaching a predefined rotation, the reverse process was carried out. The system was connected to a personal computer running the Brookfield Rheocalc 3.2 software, which controlled the Rheometer and collected the experimental shear rate and corresponding shear stress data.

Electrospinning of the PVA Compositions Loaded with GPE, NYS and CS1%

The electrospinning operation was performed at a controlled temperature and relative humidity (~22 °C and 40%). The formulations (F1 to F5) were placed in a 5 mL plastic syringe attached to a metallic needle with a 0.6 mm opening. The positive electrode of the high voltage source was connected to the needle tip, while the negative was coupled to the metallic nanofibre collector. The distance from the tip of the metallic needle to the collector metallic surface was fixed at 10 cm. The collector was previously covered with aluminium foil to facilitate the removal of the deposited nanofibre layer. The rotation velocity of the collector was fixed at 595 rpm. The electrospinning conditions were maintained constant for all experimental runs at a flow rate of 0.5 mL/h, an electrical potential of 20 kV and 3 h of electrospinning. These conditions were selected following the preliminary runs (data not shown).

Physicochemical Characterisation of the Electrospun Nanofibre Mats

After the electrospinning operation, the nanofibre mat was removed from the collector and characterised by determining the morphology, nanofibre diameter distribution, average nanofibre diameter and average surface porosity. The behaviour of the formed nanofibre mats in an aqueous medium was also evaluated through the disintegration and swelling capacity assays. The procedures used in these characterisations are presented below.

Morphology of the Electrospun Nanofibre Mats

The morphology of the electrospun nanofibre mats was evaluated through photomicrographs obtained through scanning electron microscopy (SEM). Three samples of approximately 5 × 5 mm from the electrospun nanofibre mats were fixed in aluminium sample holders with double-sided carbon conductive tape and coated with carbon and gold in Bal-Tec SCD model-050 Sputter Coater under the pressure of 0.1 mbar. The nanofibre photomicrographs were obtained using the Philip XL-30 FEG equipment (initial tests) and a Carl Zeiss scanning electron microscope mod EVO 50 (optimised formulations) at magnifications of 10 kx, 20 kx and 30 kx.

Diameter Distribution, Average Diameter and Surface Porosity of the Electrospun Nanofibre Mats

The determination of the diameter distribution, average diameter and surface porosity of the electrospun nanofibre mats was done by analysing the photomicrographs obtained through SEM with the aid of DiameterJ, an ImageJ image analysis software plug-in. DiameterJ, developed by Hotaling et al. [38, 39], is an open-source validated software used to analyse the nanofibres' diameter distribution, porosity fractions and other physical properties. The DiameterJ plug-in and its description can be found for free at the following link: <https://imagej.net/DiameterJ>. The results obtained were average values for two SEM photomicrographs of each electrospinning nanofibre mat. The nanofibres' diameter distribution allowed the SPAN determinations – $SPAN = (d_{90} - d_{10})/d_{50}$ – where d_{10} , d_{50} and d_{90} are the fibres' diameters corresponding to 10%, 50% and 90% of the distribution.

Disintegration Time, DT

The measurements of D_T were made according to the methodology described by Çay et al. [35], with some modifications. Small parts of the electrospun nanofibre mats (~1 cm × 1 cm) were carefully cut and placed in

Petri dishes. The addition of purified water was carried out dropwise using a Pasteur pipette (~22 drops or 1 ml). The disintegration behaviour was monitored through samples' pictures taken at preset intervals (monitored by a chronometer).

Swelling Ratio

The percentage swelling ratio (S_R) was determined by immersing the samples in a sufficient amount of purified water. In a watch glass, parts of the fibres were carefully cut and weighed (W_d). Drops of purified water were then deposited on the samples. Excess water was removed with filter paper, and the samples were reweighed at specified times to determine the swelled weight (W_s). S_R was calculated using Eq. (1):

$$S_R = 100 \cdot (W_s/W_d^{-1}) \quad (1)$$

Statistical Analysis

The experimental results for the pH, electrical conductivity, the nanofibres' mean diameter and surface porosity were submitted to one-way ANOVA, followed by the Tukey posthoc test ($p \leq 0.05$) to detect statistically significant differences.

Results and Discussion

Chemical Characterisation of the Concentrated Green Propolis Extract

The GPE was previously characterised by determining its HPLC–DAD profiles (HPLC fingerprint) according to the

method presented in the 'Preparation of the Concentrated Green Propolis Extract' section (Fig. 2). The comparison of the HPLC fingerprint, retention times and UV spectra of the GPE with the previous results reported by de Souza et al. [27] exhibits a high similarity for the main peaks, confirming the authenticity and quality of the GPE used. By comparing the HPLC retention times and UV spectra with those obtained for the standard substances, it was also possible to identify the compounds: 1, caffeic acid (retention time 4.02 min); 2, ferulic acid (retention time 5.40 min); and 3, cinnamic acid (retention time 14.42 min).

Potential of the Hydrogen, pH, Electrical Conductivity and Rheology of the Electrospinning and Blank Formulations

Table 1 presents the experimental values of pH and the electrical conductivity of the electrospinning formulations loaded with the active compounds and of the blank compositions (PVA/W7% and PVA/W8%, PVA/G12% and CS1%).

Potential of Hydrogen, pH

It can be seen in Table 1 that the pH and electrical conductivity of the electrospinning and blank formulations varied according to their constituents. The pH values were directly impacted by the solvents used, specifically water or the combination of glacial acid and water. Formulations with water as the solvent (F1 and F2) have a higher pH than the preparations in acetic acid (F3, F4 and F5) due to the high concentration of H⁺ ions when the mixture of water and acetic acid was used. In general, adding the actives (GPE, NYS, CS1% and mixtures) did not cause a significant change in pH value compared to the blank compositions. Although the pH changed significantly, all electrospinning

Fig. 2 Chromatographic profile of the GPE and identified compounds: 1, caffeic acid (retention time 4.02); 2, ferulic acid (retention time 5.40); and 3, cinnamic acid (retention time 14.42)

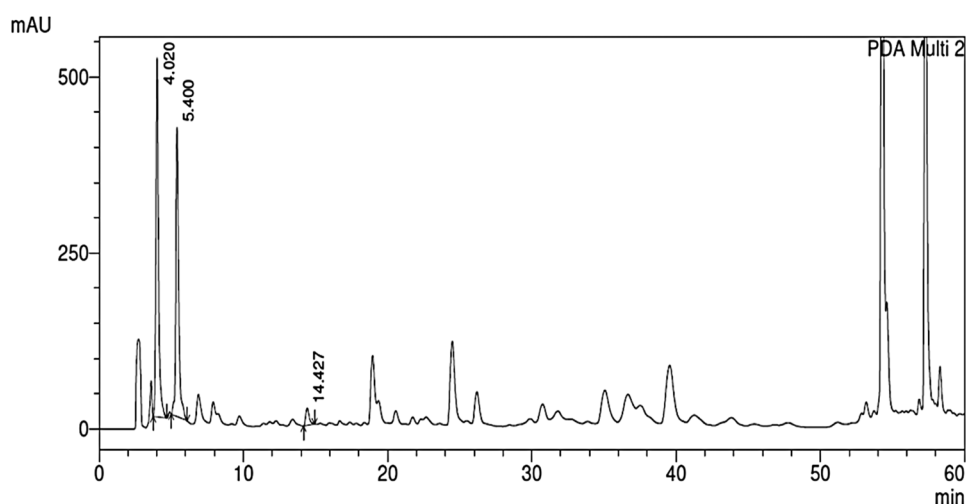


Table 1 pH and electrical conductivity of the formulations F1 to F5 and of blank compositions

Formulations (<i>F</i>)	Properties	
	pH (-)	Electrical conductivity ($\mu\text{S}/\text{cm}$)
F1: (PVA/W7% + GPE)	4.68 \pm 0.01	328.8 \pm 1.86 ^a
F2: (PVA/W8% + GPE + NYS)	4.21 \pm 0.14	326.3 \pm 0.96 ^{a,b}
F3: (PVA/G12% + CS1%)	1.39 \pm 0.03 ^c	365.0 \pm 2.95
F4: (PVA/G12% + NYS)	1.50 \pm 0.05 ^{c,d}	324.3 \pm 4.15 ^{a,b}
F5: (PVA/G12% + CS1% + NYS)	1.34 \pm 0.04 ^{c,d,e}	311.5 \pm 0.43 ^e
Blank solutions		
PVA/W7%	5.13 \pm 0.01 ^f	277.6 \pm 4.29
PVA/W8%	5.22 \pm 0.06 ^f	313.6 \pm 1.76 ^e
PVA/G 12%	1.31 \pm 0.05 ^{c,d,e}	223.0 \pm 5.88
CS1%	1.75 \pm 0.28	500.4 \pm 3.16

The same letters indicate not statistically significant ($p \leq 0.05$ – one-way ANOVA, followed by Tukey posthoc test)

formulations produced good quality electrospun nanofibre mats. Rwei and Huang [40] showed in their study with PVA solutions at various concentrations that the pH did not affect the diameters of the electrospun fibres.

Electrical Conductivity

The electrical conductivity of the solution is a relevant parameter in the electrospinning process. It indicates the charges' concentration and mobility on the surface of the electrospinning solution. A critical conductivity value must be established since the formation of fibres without defects (beads) will not occur at conductivity values that are either too low or excessively high. The migration of charges to the surface of the electrospinning formulations is almost entirely avoided for compositions with excessively low electrical conductivity. However, the conductivity can be changed by replacing the solvent system or adding ionic additives such as salts and mineral acids.

On the other hand, the Taylor cone generation and the beginning of flexural instability are impaired due to the difficulty of accumulating surface charges on the electrospinning composition drop if the conductivity is too high. Therefore, there is an ideal range of electrical conductivity values in which electrospinning is feasible, thus generating micrometric or nanometric fibres. In this range, fibre diameters tend to decrease inversely with electrical conductivity [41, 42]. Usually, the electrical conductivity values are preset for each intended preparation.

The experimental values of conductivity found in this study (Table 1) ranged from 311.5 to 500.4 $\mu\text{S}/\text{cm}$. For the blank formulations based on water (W), the conductivity ranged from 277.6 to 313.6 $\mu\text{S}/\text{cm}$ when the PVA concentration increased from 7 to 8%. Similar behaviour

was also observed by Niu et al. [43], who found an increase in conductivity (from 192.47 to 325.31 $\mu\text{S}/\text{cm}$) directly proportional to the concentration of zein (0 to 100%) in aqueous solutions. The behaviour was associated with the decrease in water content during polymer ionisation.

The electrospinning formulations loaded with the actives (F1 to F5) presented approximately similar conductivity values that were higher than the blank PVA solutions. As reported in the literature, a slight variation in the formulation composition's conductivity can be observed by adding compounds [44, 45] or increasing the polymer concentration [46].

The blank chitosan composition and composition F3, composed of PVA and chitosan, showed the highest conductivities, namely 500.4 $\mu\text{S}/\text{cm}$ and 365.0 $\mu\text{S}/\text{cm}$. Although chitosan was used in this work for the biological functionalisation of fibres, it positively affects the formation and yield of electrospun nanofibres, perhaps due to the interactions of the PVA/CS functional groups promoting the formation of hydrogen bonds in the PVA/CS membranes. These compositions are more advantageous than pure PVA, especially when used in applications as tissue supports and wound healing materials [33].

Rheology

The rheological properties of the electrospinning formulations strongly influence the electrospinning process and the properties of the electrospun nanofibres formed [22, 40, 47]. There is a direct relationship between the formulation's viscosity and the entanglement of the formed electrospun nanofibre mats. Figure 3 shows the rheograms of the electrospinning formulations used in the present work. It can be seen from the graphs presented that the rheograms of the formulations are similar, exhibiting slightly pseudoplastic behaviour, except for F4, which exhibited Newtonian behaviour. On the other hand, the rheology of the blank PVA/W and PVA/G solutions exhibited typical Newtonian behaviour. The CS composition showed a slightly thixotropic behaviour, exhibiting an area of hysteresis between the ascending and descending rheology curves with the downward curve located in an upper position.

The experimental data of shear stress as a function of shear rates for blank, CS1% solutions and compositions loaded with the bioactive compounds and CS1% solutions (blank) were fitted using the classical Ostwald-de-Waele power-law model (Eq. 2) and exhibiting an excellent agreement (traced lines in the graphs of Figs. 3 and 4).

$$\tau = K \cdot \dot{\gamma}^n \quad (2)$$

where τ is the shear stress, $\dot{\gamma}$ is the shear rate, K is the consistency index which measures the difficulty of the fluid to flow, and n is the flow index, which measures the deviation of the fluid from Newtonian behaviour. Newtonian fluid has a flow index of 1.0. Table 2 presents the parameters of the

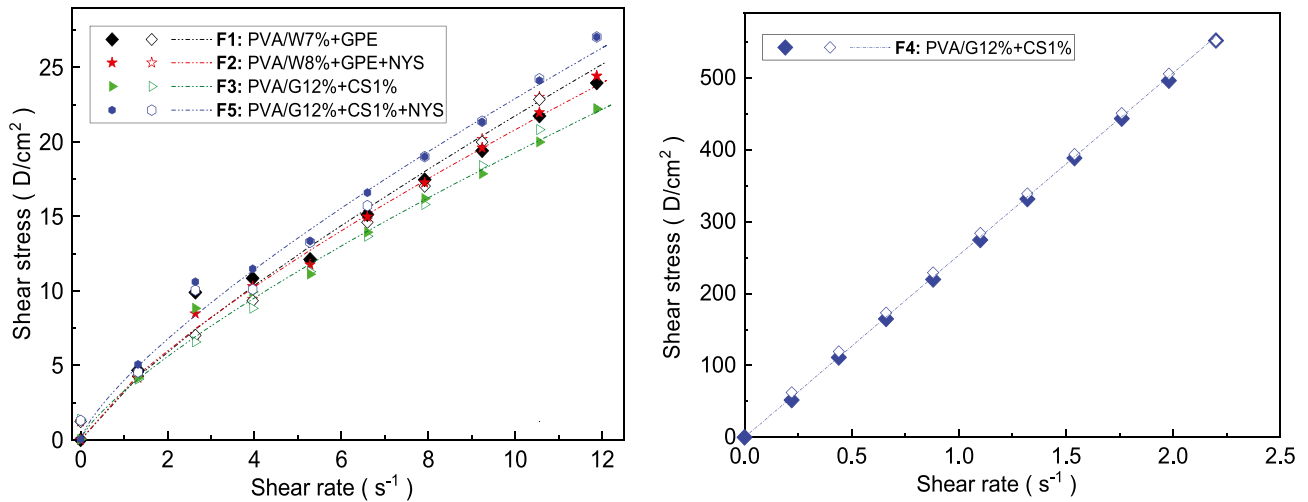


Fig. 3 Rheology of electrospinning formulations F1 to F5 – measurements obtained by increasing (solid symbols) and decreasing shear rates (open symbols)

Ostwald-de-Waele model adjusted to the rheological data of the electrospinning formulations loaded with GPE, CS and NYS (F1 to F5) and of the blank and CS1% solutions with the corresponding coefficients of determination (R^2). The value of apparent viscosity at a shear rate of 1 s^{-1} (ascending curve), similar to the value of the consistency index (Eq. 2), was used to compare the rheological behaviours of the different formulations under study.

$$\mu_{\text{ap}}^* = K \cdot \dot{\gamma}^{n-1} = K \quad (3)$$

The slight pseudoplastic behaviour that emerged in the electrospinning formulations was caused by adding the actives. Macromolecules can be organised in a state of

lower energy, such as coils. By applying the shear rate, they reorganise and orient themselves towards the flow with a decrease in apparent viscosity [24]. This behaviour applies to samples F1, F2, F3 and F5. Formulation F4 shows a remarkable increase in the consistency of the formulation, reaching a viscosity value of 253.510 P. This is caused by the simultaneous increase in the PVA concentration and changing the solvent system.

An abrupt increase in the viscosity of PVA in water and binary solvents was also observed by Rosic et al. [22] and Mahmud et al. [48] at PVA concentrations above 10% (w/v). This change can be attributed to the greater number of chain tangles and inter- and intra-molecular interactions

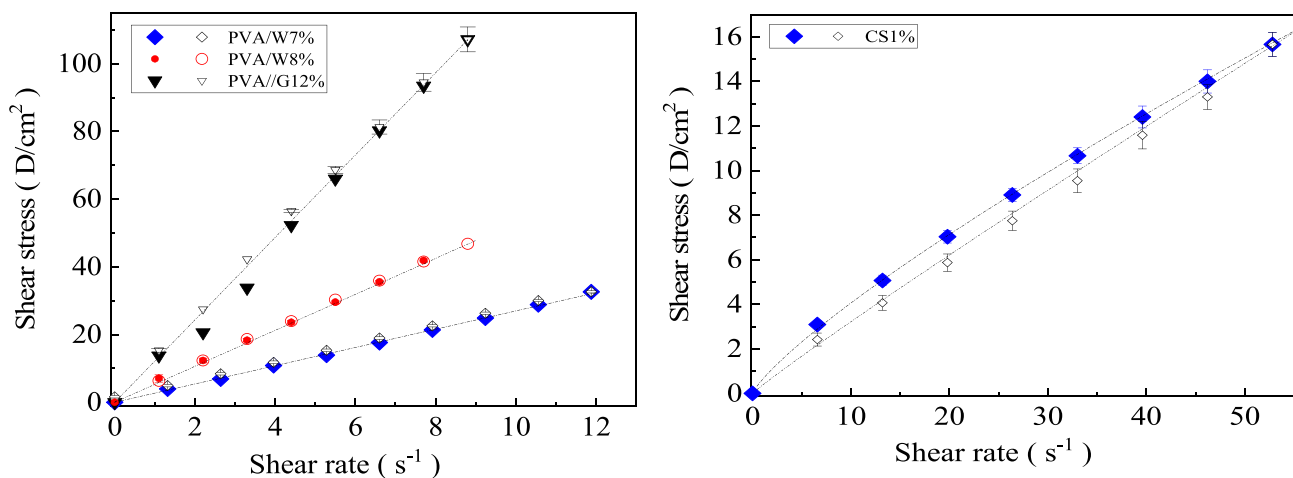


Fig. 4 Rheology of the blank PVA/W at a concentration of 7% and 8%, PVA/G12% and CS1% solutions – measurements obtained by increasing (solid symbols) and decreasing shear rates (open symbols)

Table 2 Parameters of the Ostwald-de-Waele model adjusted to the rheological data of electrospinning formulations loaded with GPE, CS1% and NYS (F1 to F5) and to the precursor compositions (blank), with the determination coefficients (R^2)

Parameter Form	μ_{ap}^a (P)	K (P.s $^{n-1}$)	n (-)	R^2 (-)
F1: (PVA/W 7%+GPE)	3.536	3.536	0.770	0.983
F2: (PVA/W8%+GPE+NYS)	3.195	3.195	0.821	0.994
F3: (PVA/G12%+CS1%)	3.281	3.281	0.769	0.998
F4: (PVA/G12%+NYS)	253.5 ^b	-	-	0.997
F5: (PVA/G12%+CS1%+NYS)	3.999	3.999	0.758	0.981
Blank solutions				
PVA/W 7%	2.695	-	-	0.995
PVA/W 8%	5.308	-	-	0.999
PVA/G 12%	129.7	-	-	0.999
CS/G 1%(i)	0.623	0.623	0.818	0.990
CS/G 1%(v)	0.363	0.363	0.948	0.990

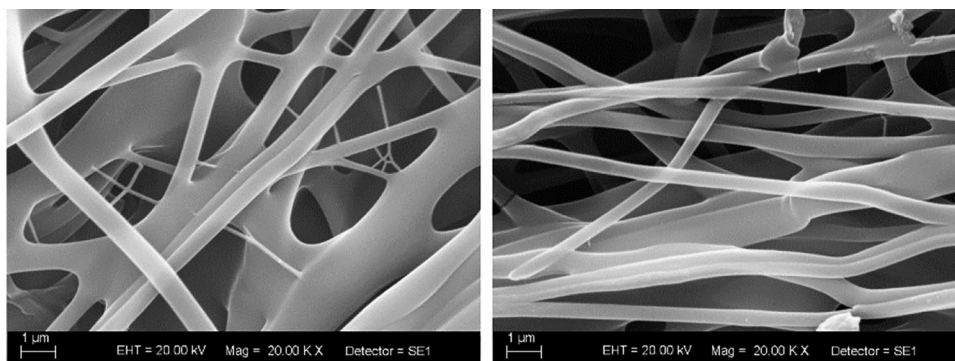
^aApparent viscosity at $\dot{\gamma}$ of $1 \text{ s}^{-1} = K \cdot \dot{\gamma}^{n-1} = K$

^bNewtonian behaviour

of the polar -OH groups of PVA in the system. Guerrini et al. [47] also observed pseudoplastic behaviour in 12.4% PVA solutions in water, while Goncalves et al. [34] faced difficulty in electrospinning formulations containing PVA and chitosan due to their very high viscosities.

Regarding the addition of active compounds, the combination GPE+NYS decreases the viscosity of the PVA/W8% blank solution from 5308 to 3195 P. Adding CS1% to the PVA/G12% solution leads to a rheological behaviour similar to the PVA/W electrospinning formulations (F1 and F2), perhaps due to a dilution effect since a 50:50 PVA/G12%:CS1% ratio was used. Although the rheology of compositions F1, F2, F3 and F5 showed almost similar behaviour, the characteristics of the nanofibre mats changed significantly. This trend reinforces the direct impact of the interaction between the constituents of the electrospinning formulation on the nanofibre mat structure.

Fig. 5 SEM photomicrographs of the electrospun nanofibres mat based on PVA/W7% and PVA/W8% formulations loaded with GPE (F1) and GPE+NYS (F2), magnification of 20 kx



F1

F2

Morphology of the Electrospun Nanofibres

Figures 5 and 6 show SEM photomicrographs of the electrospun nanofibres formed from PVA/W7% and PVA/W8% formulations loaded with GPE and GPE+NYS (respectively, F1 and F2) and PVA/G12% loaded with CS1%, NYS and CS+NYS (respectively, F3 to F5), at a magnification of 20 kx. It can be seen from the figures that the active therapeutic agents in the solutions affected the morphological fibre characteristics such as their appearance, diameters and entanglement significantly. The images do not evidence the presence of granules, beads or other defects.

Diameter and Surface Porosity of the Electrospun Nanofibre Mats

The diameter distribution, average diameter and the average surface porosity of the electrospun nanofibre mats were determined through image analysis of the SEM photomicrographs. From the results, it was possible to plot the differential and accumulated distribution of nanofibre diameters (Figs. 7 and 8) for the electrospun nanofibres based on PVA/W formulations loaded with GPE and GPE+NYS (F1 and F2) and on PVA/G12% compositions loaded with CS, NYS and CS+NYS (F3 to F5).

The data plotted in Figs. 7 and 8 allowed for the determination of the average fibre diameter ($d_{average}$), the distribution parameters d_{10} , d_{50} and d_{90} , and the distribution SPAN, given by $SPAN = (d_{90} - d_{10})/d_{50}$. The parameters d_{10} , d_{50} and d_{90} refer to the fibres' diameters corresponding to 10%, 50% and 90% of the distribution. Table 3 summarises the results obtained with the average porosity values ($\epsilon_{average}$) estimated by image analysis.

The electrospun nanofibre mats show significant morphological differences. The nanofibre samples F1 and F2 exhibited lower tangles and misshapen distribution than samples F3, F4 and F5. The morphology suggests a fused fibre format (mainly for the F1 sample), thus revealing the

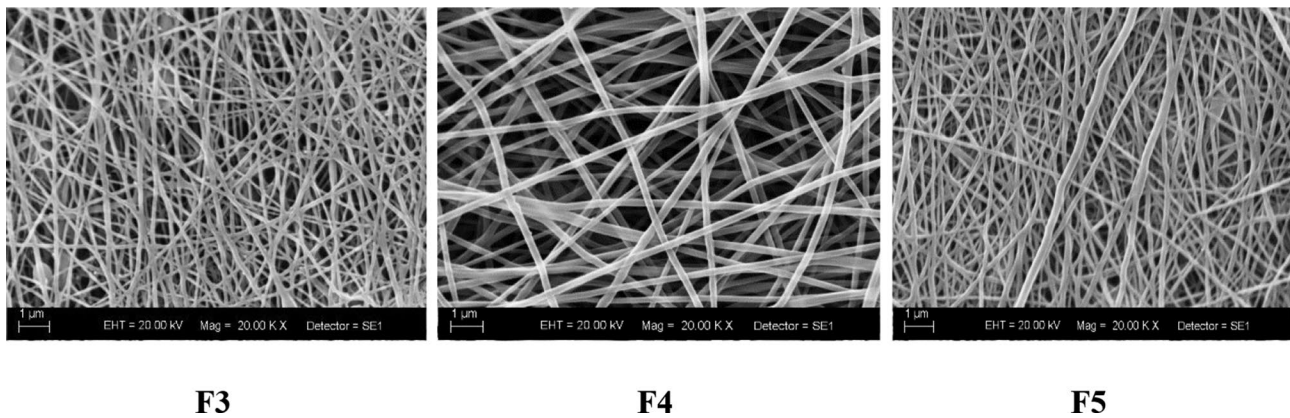


Fig. 6 SEM photomicrographs of the electrospun nanofibres mat based on PVA/G12% formulations loaded with CS1% (**F3**), NYS (**F4**) and CS +NYS (**F5**), magnification of 20 kx

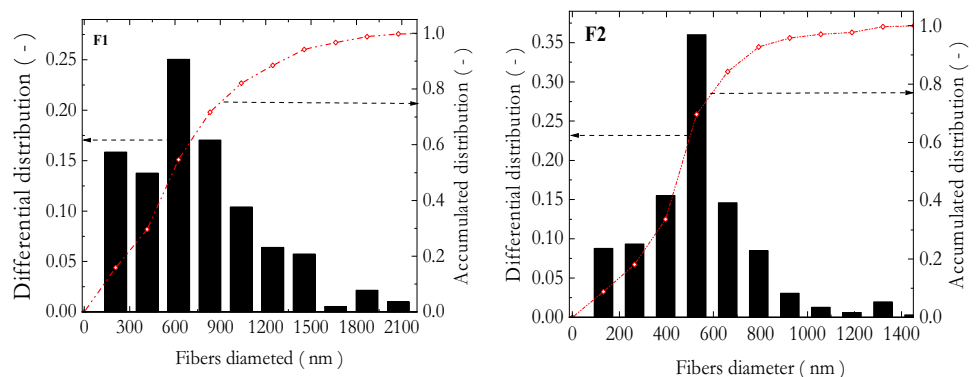
presence of interconnections, most notably in the F2 sample. The mean diameters found (Table 3) for these fibres were the largest, 684.5 ± 13.7 (F1) and 476.2 ± 10.7 (F2). The diameter distribution parameters (Table 3) indicate greater diameters in d_{90} due to the proportion of fibres in the form of wider ribbons, tending to become larger than the narrow ones. Although these features are common to both fibres, they are more prominent in F1. For sample F2, the association of GPE and NYS significantly altered the fibres' morphological characteristics, exhibiting a decrease in fibre diameter on the connection points (interconnections). There are reports of a significant increase in the diameter of electrospun fibres loaded with propolis and other natural compounds, including the microfibre formation, depending on the concentration of actives in the formulation [49, 50]. However, studies involving associations between natural and synthetic actives in nanofibres still demand more experimental studies.

The propolis concentration in the formed nanofibre mats reached 30% (w/v) in both the PVA/W7% and PVA/W8% solutions, a concentration also used by Razavizadeh and Niazmand [50]. The lower volatility of the F1 and F2 electrospinning formulations loaded with GPE can be

pointed out as interfering with the morphology of the nanofibre mats. The material subjected to electrospinning might remain slightly moist when it reaches the collector surface, making the fibres wider when they are deposited wet on top of each other. The low solubility of propolis, combined with its adhesive propensity, can favour the connection of fibres at the crossing points. These points can represent an excellent reinforcement element for the formed fibres and may be desirable for application as wound dressings [51]. Perhaps, the decrease of the GPE concentration in the polymer solution can improve the morphology and diminish the size of the propolis nanofibres. Kim et al. [51] found that the measured diameters were uniform and the morphological changes were minimised for small propolis concentrations in the electrospinning formulations.

Nanofibres loaded with CS1% and NYS (F3, F4 and F5) showed a predominance of well-defined entanglements, random orientation and the smallest diameters. The solution composition (polymer concentration and solvent system) and the addition of CS1% (F3 and F5) had a positive effect on processability and fibres' morphology and diameter. It was possible to obtain elegant nanofibres

Fig. 7 Differential and accumulated diameter distribution of the electrospun nanofibres mat based on PVA/W formulations loaded with GPE and GPE +NYS (respectively, **F1** and **F2**), magnification of 20 kx



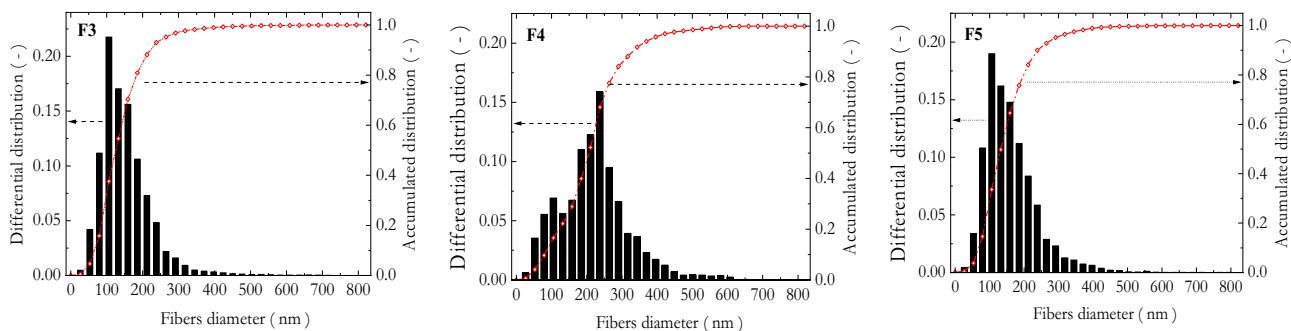


Fig. 8 Differential and accumulated diameter distribution, SPAN, average diameter and average surface porosity of the electrospun nanofibres mat based on 12% PVA/G composition loaded with CS1%, NYS and CS1% + NYS (respectively, **F3** to **F5**), magnification of 20 kx

from the more viscous PVA/G12% + NYS formulation (**F4**) which exhibits a Newtonian rheological behaviour. In addition, the presence of 70% acetic acid in the solvent system and NYS's addition greatly increased the **F4**'s formulation consistency, forming nanofibres of a smaller diameter (220.9 ± 9.3). Shibata [16] reported an increase of the nanofibre's diameters when the PVA concentration was in an aqueous solution up to 10% w/v, with a slight tendency to reduce from the 12% PVA concentration. These researchers also propose the occurrence of an arrangement of the PVA molecules in solution according to the concentration, showing that they can orient themselves in the direction of the applied electric field, allowing for complete elongation during electrospinning, in addition to the formation of defect-free fibres of adequate diameters. For Mahmud et al. [48], the smallest diameters were obtained from formulations with 20% glacial acetic acid:water, at concentrations of PVA of 7%, 10% and 15%.

Chitosan can be used both as a thickener for PVA solutions, improving the morphology [52], and for the biological functionalisation of nanofibre mats, as proposed in this study. However, when dissolved in an acidic medium, chitosan assumes a polyelectrolyte behaviour, increasing the charge density on the drop's surface during electrospinning, reducing the nanofibre diameter [53]. In the micrographs of **F3** and **F5**, we can see the smallest and

closest diameters. With the addition of the antimicrobial nystatin to **F5**, there was a slight increase in nanofibre diameter.

This trend was also observed by Taepaiboon et al. [7] during the production of PVA electrospun nanofibres loaded with four model drugs: sodium salicylate, sodium diclofenac, indomethacin and naproxen. The authors found that the morphology of the nanofibres was directly affected by the properties of the polymer solution and the type of model drug added.

Regarding the surface porosity of the electrospun nanofibre mats, it can be observed that the presence of larger and smaller fibres, as observed in **F1** and **F2**, resulted in good pore size distribution with high interconnectivity. This result was also observed for the **F4** electrospun nanofibre sample. The size of the pores can be directly related to the fibre diameter, which can impact the interactions between the electrospun matrix with bacteria, fungi and other living cells. Nanofibres exhibit greater cell adhesion and proliferation advantages, whereas microfibres are ideal for providing larger pores and promoting cell infiltration [53, 54]. Therefore, the presence of micro and nanofibres can be advantageous, taking into account the positive characteristics inherent to each of them. The formed materials have excellent properties linked to their use in smart dressings.

Table 3 Diameter distribution parameters (d_{mean} , d_{10} , d_{50} , d_{90} and SPAN) and mean porosity (eaverage) of the electrospun nanofibres mat based on electrospinning formulations **F1** to **F5**

Formulations	Parameters					
	d_{mean} (nm)	d_{10} (nm)	d_{50} (nm)	d_{90} (nm)	SPAN (-)	ϵ_{mean} (-)
F1: (PVA/W 7% + GPE)	684.5 ± 13.7	139.4	585.3	1307.5	2.0	0.50 ± 0.05 ^a
F2: (PVA/W8% + GPE + NYS)	476.2 ± 10.7	155.8	456.3	748.0	1.3	0.41 ± 0.02 ^b
F3: (PVA/G12% + CS1%)	151.5 ± 7.7 ^c	68.5	126.1	225.9	1.2	0.29 ± 0.04 ^c
F4: (PVA/G12% + NYS)	220.9 ± 9.3	81.3	205.3	332.1	1.2	0.43 ± 0.02 ^{a,b}
F5: (PVA/G12% + CS1% + NYS)	160.7 ± 7.6 ^c	79.1	132.0	238.2	1.2	0.31 ± 0.02 ^c

The same letters indicate not statistically significant ($p \leq 0.05$ – one-way ANOVA is generally followed by Tukey posthoc test)

Disintegration Time and Swelling Ratio of the Electrospun Nanofibre Mats

The evaluation of the behaviour of the electrospun nanofibre mats in an aqueous environment was undertaken as their disintegration time and swelling capacity are of great importance when it is intended to apply them as dressings for chronic wounds or even in the topical or mucosal delivery of active ingredients. Figure 9 shows the disintegration behaviour of the electrospun nanofibres based on the PVA/W formulations loaded with GPE and GPE + NYS (F1 and F2) and on the PVA/G12% compositions loaded with CS, NYS and CS + NYS (F3 to F5).

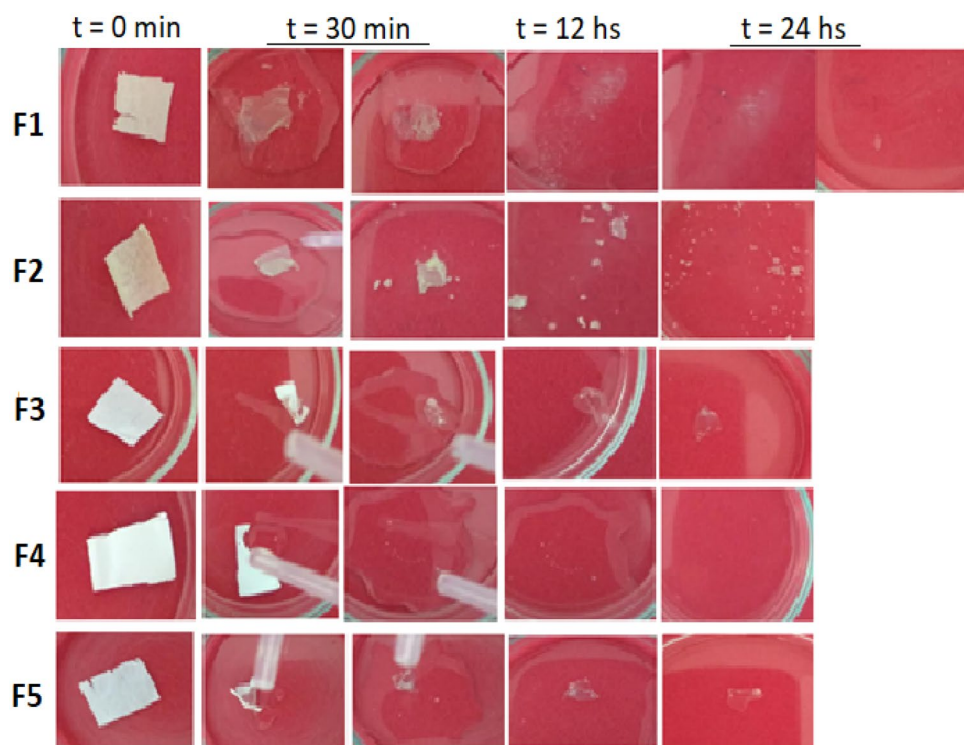
Nanofibres composed of PVA are expected to present predominantly hydrophilic characteristics since PVA is a water-soluble polymer. The shape and disintegration time of nanofibre samples F1, F2 and F4 point to this aspect, showing an almost immediate breakage of the mats after contact with water. For sample F4, the disintegration was almost instantaneous (~2 s), while it was nearly 15 min for samples F1 and F2. Small fragments were observed after the disintegration of samples F1 and F2, which remained 24 h later. Nanofibre samples F3 and F5 showed a change in appearance when in contact with water, behaving like “gel” after absorbing water, possibly linked to the chitosan presence in their composition. After 12 h of the test, it was possible to observe the presence of small fragments in the F1 and F2 nanofibre samples and the undissolved parts of F3 and F5.

Compatibility with a humid environment is considered to be an advantage in terms of the materials proposed for use in wound dressings, as healing occurs more efficiently in a dry environment [55]. Upon the dissolution of samples F1, F2 and F4, it is remarkable that the water quickly broke the structure of the nanofibre mats composed of PVA, allowing for the quick release of the actives. The small fragments observed during the tests with samples F1 and F2 may be related to GPE, a resinous compound with low solubility and NYS, which is practically insoluble in water. Nystatin, an antifungal drug of the polyene class, is not absorbed through the gastrointestinal tract, being commonly administered topically, and through the mucosa (e.g. buccal and vaginal) [56]. The external use of propolis for the treatment of oral, skin and genital diseases is well described in the excellent review reported by Sung et al. [57]. Currently, Berreta et al. [58] reported the internal use of propolis to be a tool for combating SARS-COV-2's action mechanisms.

In the study by Adomaviciute et al. [59], it was found that the structures of the nano and microfibres of PVP added with propolis and silver nanoparticles presented visual disintegration and dissolution up to 10 min. The water was also able to break the mats immediately after contact. The release of fragments was observed at different stages of dissolution, as in this study.

In samples with PVA and CS, dissolution was slow and incomplete due to the interaction of PVA with the polysaccharide chitosan. This feature is also interesting as it highlights the possibility of the absorption of exudates as

Fig. 9 Disintegration behaviour of the electrospun nanofibres based on PVA/W compositions loaded with GPE and GPE + NYS (respectively, F1 and F2) and on PVA/G12% compositions loaded with CS, NYS and CS + NYS (respectively, F3 to F5)



it tends to swell when immersed in a humid environment. A measure was calculated to verify the swelling ratio for the samples that remained insoluble, specifically F3 and F5. The result was 924% (F3) and 1100% (F4) at the end of 8 h of immersion in an aqueous environment. Archana et al. [60] found maximum swelling ratios of 1215% in a pH 2 buffer and 900% in a pH 7 buffer for chitosan, pectin and TiO₂ nanofibres. Generally speaking, the sample with the highest swelling ratio will have the highest surface area/volume ratio.

The wettability and hydrophilicity added to the greater swelling capacity of the nanofibres provided by the addition of CS can favour the absorption of exudates in the wound beds and can also be used as an innovative delivery system for the incorporated active ingredients. There is a positive relationship between better water absorption by the fibres that exhibit a good presence of pores. Zhang et al. [61] studied PVA/chitosan membranes and observed the best morphology of PVA/CS nanofibres with a higher proportion of PVA (80:20). The membranes' high surface volume and porosity are linked to a greater propensity to absorb water. Herein, we have demonstrated that a PVA/CS ratio of 50:50 in samples F3 and F5 provided a product with high water absorption capacity. This result is promising since membranes with greater water absorption and swelling capacity are suitable for application as a matrix for wound and burn dressings. In addition, the electrospinning compositions developed were very stable, confirming the compatibility between the polymers and active ingredients used. The constituents of the electrospinning compositions are biodegradable and biocompatible, non-toxic, water-based, promptly available and low costs. These advantages show the technical and economic feasibility of the nanofibres developed here as a matrix for innovative wound dressings, which is the subject of ongoing studies, which include in vitro and ex vivo assays.

Conclusions

It is feasible to produce electrospun biodegradable micro and nanofibre mats from PVA, incorporated with green propolis extract (GPE), nystatin (NYS) and chitosan (CS) – alone or in mixtures. The properties of electrospun nanofibres are significantly affected by the constituents and physicochemical properties of the electrospinning formulations, such as pH, electrical conductivity and rheology. Adding chitosan with the concentrated acetic acid positively affects the properties of electrospun nanofibres, resulting in fibres of small diameter with reduced defects and high swelling capacity. These characteristics are ideal for applying the produced PVA/CS nanofibre mats as a novel material for wound and burn dressings or for transdermal delivery systems.

Acknowledgements The authors would like to acknowledge the Coordination of Superior Level Staff Improvement (CAPES), Grant N° 88887505019/2020-00, São Paulo Research Foundation (FAPESP), Grants 2016/20500-6 and 2018/26069-0, and the National Council of Technological and Scientific Development (CNPq) for their financial support.

Declarations

Conflict of Interest The authors declare no competing interests.

References

- Huebsch N, Mooney DJ. Inspiration and application in the evolution of biomaterials. *Nature*. 2009;462:426–32. Available from: <http://www.nature.com/articles/nature08601>.
- Stace ET, Mouthuy P-A, Carr AJ, Ye HC. Biomaterials: electrospinning. *Compr Biotechnol*. Elsevier; 2019; p. 424–41. Available from: <https://linkinghub.elsevier.com/retrieve/pii/B9780444640468002731>.
- Vrbata P, Berka P, Stránská D, Doležal P, Lázníček M. Electrospinning of diosmin from aqueous solutions for improved dissolution and oral absorption. *Int J Pharm*. 2014;473:407–13. Available from: <https://linkinghub.elsevier.com/retrieve/pii/S037851731400516X>.
- Shirata MMF, Campos PMBGM. Importance of texture and sensorial profile in cosmetic formulations development. *Surg Cosmet Dermatology*. 2016;8. Available from: <http://www.surgicocosmetic.org.br/detalhe-artigo/495/Importancia-do-perfil-de-textura-e-sensorial-no-desenvolvimento-de-formulacoes-cosmeticas>.
- Li N, Zhang ZJ, Li XJ, Li HZ, Cui LX, He DL. Microcapsules biologically prepared using *Perilla frutescens* (L.) Britt. essential oil and their use for extension of fruit shelf life. *J Sci Food Agric*. 2018;98:1033–41.
- Sandri G, Rossi S, Bonferoni MC, Caramella C, Ferrari F. Electrospinning technologies in wound dressing applications. *Ther Dressings Wound Heal Appl*. Wiley; 2020. p. 315–36. Available from: <https://doi.org/10.1002/9781119433316.ch14>.
- Taepaiboon P, Rungsardthong U, Supaphol P. Drug-loaded electrospun mats of poly(vinyl alcohol) fibres and their release characteristics of four model drugs. *Nanotechnology*. 2006;17:2317–29. Available from: <https://doi.org/10.1088/0957-4484/17/9/041>.
- Coppari S, Ramakrishna S, Teodori L, Albertini MC. Cell signalling and biomaterials have a symbiotic relationship as demonstrated by a bioinformatics study: the role of surface topography. *Curr Opin Biomed Eng*. 2021;17:100246. Available from: <https://linkinghub.elsevier.com/retrieve/pii/S2468451120300416>.
- Huang ZM, Zhang YZ, Kotaki M, Ramakrishna S. A review on polymer nanofibers by electrospinning and their applications in nanocomposites. *Compos Sci Technol Elsevier BV*. 2003;63:2223–53.
- Aslam M, Kalyar MA, Raza ZA. Polyvinyl alcohol: a review of research status and use of polyvinyl alcohol based nanocomposites. *Polym Eng Sci*. 2018;58:2119–32. Available from: <https://doi.org/10.1002/pen.24855>.
- Jiang S, Liu S, Feng W. PVA hydrogel properties for biomedical application. *J Mech Behav Biomed Mater*. 2011;4:1228–33. Available from: <https://linkinghub.elsevier.com/retrieve/pii/S1751616111000786>.
- Sheskey PJ, Hancock BC, Moss GP, Goldfarb DJ. *Handbook of pharmaceutical excipients*. 9th ed. Foster City, USA: Pharmaceutical Press; 2020.
- Zeinali T, Alemzadeh E, Zarban A, Khorashadizadeh M, Ansarifard E. Fabrication and characterization of jujube extract-loaded electrospun polyvinyl alcohol nanofiber for strawberry

- preservation. *Food Sci Nutr*. Wiley-Blackwell; 2021;9:6353–61. Available from: <https://onlinelibrary.wiley.com/doi/full/10.1002/fsn3.2601>.
14. Rafeian Isfahani F, Tavanai H, Morshed M. Release of *Aloe vera* from Electrospun Aloe vera-PVA Nanofibrous Pad. *Fibers Polym*. 2017;18:264–71.
 15. Shahid MA, Khan MS. Preparation and characterization of electrospun nanofiber membrane from polyvinyl alcohol loaded with *Glycyrrhiza glabra* extract. *Polym Polym Compos*. 2022;30:1–8. Available from: <https://us.sagepub.com/en-us/nam/open-access-at-sage>.
 16. Shibata T, Yoshimura N, Kobayashi A, Ito T, Hara K, Tahara K. Emulsion-electrospun polyvinyl alcohol nanofibers as a solid dispersion system to improve solubility and control the release of probucol, a poorly water-soluble drug. *J Drug Deliv Sci Technol*. 2022;67:102953. Available from: <https://linkinghub.elsevier.com/retrieve/pii/S177322472100633X>.
 17. Kenry, Lim CT. Nanofiber technology: current status and emerging developments. *Prog Polym Sci*. 2017;70:1–17. Available from: <https://linkinghub.elsevier.com/retrieve/pii/S0079670017300692>.
 18. Haider A, Haider S, Kang I-K. A comprehensive review summarizing the effect of electrospinning parameters and potential applications of nanofibers in biomedical and biotechnology. *Arab J Chem*. 2018;11:1165–88. Available from: <https://linkinghub.elsevier.com/retrieve/pii/S1878535215003275>.
 19. Gong L, Li T, Chen F, Duan X, Yuan Y, Zhang D, et al. An inclusion complex of eugenol into β -cyclodextrin: preparation, and physicochemical and antifungal characterization. *Food Chem Elsevier*. 2016;196:324–30.
 20. Li Z, Wang C. Effects of working parameters on electrospinning. Springer, Berlin, Heidelberg; 2013 [cited 2020 Aug 8]. p. 15–28. Available from: https://doi.org/10.1007/978-3-642-36427-3_2.
 21. Bhardwaj N, Kundu SC. Electrospinning: a fascinating fiber fabrication technique. *Biotechnol Adv*. 2010;28:325–47. Available from: <https://linkinghub.elsevier.com/retrieve/pii/S0734975010000066>.
 22. Rošić R, Pelipenko J, Kristl J, Kocbek P, Bešter-Rogač M, Baumgartner S. Physical characteristics of poly (vinyl alcohol) solutions in relation to electrospun nanofiber formation. *Eur Polym J*. 2013;49:290–8.
 23. Okutan N, Terzi P, Altay F. Affecting parameters on electrospinning process and characterization of electrospun gelatin nanofibers. *Food Hydrocoll*. 2014;39:19–26. Available from: <https://linkinghub.elsevier.com/retrieve/pii/S0268005X13004062>.
 24. Arkan HK, Solak HH. Propolis Extract-PVA Nanocomposites of textile design: antimicrobial effect on gram positive and negative bacterias. *Int J Second Metab*. 2017;4:218–24. Available from: <https://doi.org/10.21448/ijsm.371563>.
 25. Elsabee MZ, Naguib HF, Morsi RE. Chitosan based nanofibers, review. *Mater Sci Eng C*. 2012;32:1711–26. Available from: <https://linkinghub.elsevier.com/retrieve/pii/S0928493112002135>.
 26. Kristanc L, Božič B, Jokhadar ŠZ, Dolenc MS, Gomišček G. The pore-forming action of polyenes: from model membranes to living organisms. *Biochim Biophys Acta - Biomembr*. 2019;1861:418–30. Available from: <https://linkinghub.elsevier.com/retrieve/pii/S0005273618303444>.
 27. de Sousa JPB, Bueno PCP, Gregório LE, da Silva Filho AA, Furtado NAJC, de Sousa ML, et al. A reliable quantitative method for the analysis of phenolic compounds in Brazilian propolis by reverse phase high performance liquid chromatography. *J Sep Sci*. 2007;30:2656–65. Available from: <https://doi.org/10.1002/jssc.200700228>.
 28. Braga GK. Determinação das especificações do processo “spray drying” na obtenção de micropartículas biodegradáveis para liberação sustentada de princípios ativos com aplicações odontológica. [Ribeirão Preto]: Universidade de São Paulo; 2005. Available from: <http://www.teses.usp.br/teses/disponiveis/60/60131/tde-09012009-144551/>.
 29. Benelli L, Cortés-Rojas DF, Souza CRF, Oliveira WP. Fluid bed drying and agglomeration of phytopharmaceutical compositions. *Powder Technol*. 2015;273:145–53. Available from: <https://linkinghub.elsevier.com/retrieve/pii/S0032591014010043>.
 30. Springfield EP, Eagles PKF, Scott G. Quality assessment of South African herbal medicines by means of HPLC fingerprinting. *J Ethnopharmacol*. 2005;101:75–83. Available from: <https://linkinghub.elsevier.com/retrieve/pii/S0378874105002448>.
 31. Cortés-Rojas DF, Chagas-Paula DA, Da Costa FB, Souza CRF, Oliveira WP. Bioactive compounds in *Bidens pilosa* L. populations: a key step in the standardization of phytopharmaceutical preparations. *Rev Bras Farmacogn*. 2013;23:28–35. Available from: <https://linkinghub.elsevier.com/retrieve/pii/S0102695X13700036>.
 32. Paipitak K, Pornpra T, Mongkontalang P, Techitdheer W, Pecharapa W. Characterization of PVA-chitosan nanofibers prepared by electrospinning. *Procedia Eng*. 2011 [cited 2022 Aug 15];8:101–5. Available from: www.sciencedirect.com.
 33. Li T-T, Yan M, Zhong Y, Ren H-T, Lou C-W, Huang S-Y, et al. Processing and characterizations of rotary linear needleless electrospun polyvinyl alcohol(PVA)/chitosan(CS)/graphene(Gr) nanofibrous membranes. *J Mater Res Technol*. Elsevier; 2019 [cited 2022 Aug 16];8:5124–32. Available from: <https://linkinghub.elsevier.com/retrieve/pii/S2238785419303217>.
 34. Gonçalves RP, Ferreira WH, Gouvêa RF, Andrade CT. Effect of chitosan on the properties of electrospun fibers from mixed poly(vinyl alcohol)/chitosan solutions. *Mater Res* 2017 [cited 2020 Aug 8];20:984–93. Available from: http://www.scielo.br/scielo.php?script=sci_arttext&pid=S1516-14392017000400984&lng=en&tlang=en.
 35. Çay A, Mirafteb M, Perrin Akçakoca Kumbasar E. Characterization and swelling performance of physically stabilized electrospun poly(vinyl alcohol)/chitosan nanofibres. *Eur Polym J*. Pergamon; 2014;61:253–62. Available from: <https://linkinghub.elsevier.com/retrieve/pii/S0014305714003693>.
 36. Gupta D, Jassal M, Agrawal AK. The electrospinning behavior of poly(vinyl alcohol) in DMSO–water binary solvent mixtures. *RSC Adv Royal Soc Chem*. 2016;6:102947–55. Available from: <https://pubs.rsc.org/en/content/articlehtml/2016/ra/c6ra15017a>.
 37. Geng X, Kwon OH, Jang J. Electrospinning of chitosan dissolved in concentrated acetic acid solution. *Biomaterials Elsevier BV*. 2005;26:5427–32.
 38. Hotaling NA, Bharti K, Kriel H, Simon CG. Dataset for the validation and use of DiameterJ an open source nanofiber diameter measurement tool. *Data Br*. 2015;5:13–22. Available from: <https://linkinghub.elsevier.com/retrieve/pii/S2352340915001316>.
 39. Hotaling NA, Bharti K, Kriel H, Simon CG. DiameterJ: a validated open source nanofiber diameter measurement tool. *Biomaterials*. 2015;61:327–38. Available from: <https://linkinghub.elsevier.com/retrieve/pii/S0142961215004652>.
 40. Rwei S-P, Huang C-C. Electrospinning PVA solution-rheology and morphology analyses. *Fibers Polym*. Springer; 2012;13:44–50. Available from: <https://doi.org/10.1007/s12221-012-0044-9>.
 41. Xue J, Wu T, Dai Y, Xia Y. Electrospinning and electrospun nanofibers: methods, materials, and applications. *Chem Rev*. 2019;119:5298–415.
 42. Goy RC, Britto D de, Assis OBG. A review of the antimicrobial activity of chitosan. *Polímeros*. 2009;19:241–7. Available from: http://www.scielo.br/scielo.php?script=sci_arttext&pid=S0104-14282009000300013&lng=en&tlang=en.
 43. Niu B, Zhan L, Shao P, Xiang N, Sun P, Chen H, et al. Electrospinning of zein-ethyl cellulose hybrid nanofibers with improved water resistance for food preservation. *Int J Biol Macromol*. 2020;142:592–9. Available from: <https://linkinghub.elsevier.com/retrieve/pii/S0141813019372393>.
 44. Tuğcu-Demiröz F, Saar S, Tort S, Acartürk F. Electrospun metronidazole-loaded nanofibers for vaginal drug delivery. *Drug Deliv*

- Ind Pharm. 2020;46:1015–25. Available from: <https://doi.org/10.1080/03639045.2020.1767125>.
45. Sadeghi A, Pezeshki-Modaress M, Zandi M. Electrospun polyvinyl alcohol/gelatin/chondroitin sulfate nanofibrous scaffold: fabrication and in vitro evaluation. *Int J Biol Macromol*. 2018;114:1248–56. Available from: <https://linkinghub.elsevier.com/retrieve/pii/S0141813017351462>.
 46. Nagy ZK, Nyul K, Wagner I, Molnar K, Marosi G. Electrospun water soluble polymer mat for ultrafast release of Donepezil HCl. *Express Polym Lett*. 2010;4:763–72. Available from: <http://www.expresspolymlett.com/letolt.php?file=EPL-0001669&mi=c>.
 47. Guerrini LM, Branciforti MC, Bretas RES, Oliveira MP de. Eletrofição do poli (álcool vinílico) via solução aquosa. *Polímeros*. 2006;16:286–93. Available from: http://www.scielo.br/scielo.php?script=sci_arttext&pid=S0104-14282006000400007&lng=pt&tng=pt.
 48. Mahmud MM, Perveen A, Matin MA, Arafat MT. Effects of binary solvent mixtures on the electrospinning behavior of poly (vinyl alcohol). *Mater Res Express*. 2018;5:115407. Available from: <https://doi.org/10.1088/2053-1591/aad1f1f>.
 49. Rebia RA, binti Sadon NS, Tanaka T. Natural antibacterial reagents (centella, propolis, and hinokitiol) loaded into poly[(R)-3-hydroxybutyrate-co-(R)-3-hydroxyhexanoate] composite nanofibers for biomedical applications. *Nanomaterials*. 2019;9:1665. Available from: <https://www.mdpi.com/2079-4991/9/12/1665>.
 50. Razavizadeh BM, Niazmand R. Characterization of polyamide-6/propolis blended electrospun fibers. *Heliyon*. 2020;6:e04784. Available from: <https://linkinghub.elsevier.com/retrieve/pii/S2405844020316273>.
 51. Kim JI, Pant HR, Sim H-J, Lee KM, Kim CS. Electrospun propolis/polyurethane composite nanofibers for biomedical applications. *Mater Sci Eng C*. 2014;44:52–7. Available from: <https://linkinghub.elsevier.com/retrieve/pii/S0928493114004809>.
 52. Li L, Hsieh Y-L. Chitosan bicomponent nanofibers and nanoporous fibers. *Carbohydr Res*. 2006;341:374–81. Available from: <https://linkinghub.elsevier.com/retrieve/pii/S0008621505005379>.
 53. Lanno GM, Ramos C, Preem L, Putrins M, Laidmaē I, Tenson T, et al. Antibacterial porous electrospun fibers as skin scaffolds for wound healing applications. *ACS Omega*. *Am Chem Soc*. 2020;5:30011–22. Available from: <https://doi.org/10.1021/acsomega.0c04402>.
 54. Wu J, Hong Y. Enhancing cell infiltration of electrospun fibrous scaffolds in tissue regeneration. *Bioact Mater*. 2016;1:56–64. Available from: <https://linkinghub.elsevier.com/retrieve/pii/S2452199X16300135>.
 55. Franco D, Gonçalves LF. Feridas cutâneas: a escolha do curativo adequado. *Rev Col Bras Cir. Colégio Brasileiro de Cirurgiões*. 2008 [cited 2021 Nov 10];35:203–6. Available from: <http://www.scielo.br/rbc/a/LFCNqqNQH9zZqjJgNLCYkws/?lang=pt>.
 56. Bondaryk M, Kurzątkowski W, Staniszevska M. Antifungal agents commonly used in the superficial and mucosal candidiasis treatment: mode of action and resistance development. *Adv Dermatol Allergol*. 2013;5:293–301. Available from: <https://doi.org/10.5114/pdia.2013.38358>.
 57. Sung S-H, Choi G-H, Lee N-W, Shin B-C. External use of propolis for oral, skin, and genital diseases: a systematic review and meta-analysis. *Evidence-Based Complement Altern Med*. 2017;2017:1–10. Available from: <https://www.hindawi.com/journals/ecam/2017/8025752/>.
 58. Berretta AA, Silveira MAD, Córdor Capcha JM, De Jong D. Propolis and its potential against SARS-CoV-2 infection mechanisms and COVID-19 disease. *Biomed Pharmacother*. 2020;131:110622. Available from: <https://linkinghub.elsevier.com/retrieve/pii/S0753332220308155>.
 59. Adomavičiūtė E, Stanys S, Žilius M, Briedis V. Formation and analysis of electrospun nonwoven mats from bicomponent PVA/aqueous propolis nano-microfibres. *Fibres Text East Eur. Łukasiewicz Res Netw- Inst Biopolym Chem Fibres*. 2015 [cited 2021 Nov 10];23:35–41. Available from: <http://220.indexcopernicus.com/abstracted.php?level=5&ICID=1161754>.
 60. Archana D, Dutta J, Dutta PK. Evaluation of chitosan nano dressing for wound healing: characterization, in vitro and in vivo studies. *Int J Biol Macromol*. *Int J Biol Macromol*. 2013 [cited 2021 Nov 10];57:193–203. Available from: <https://pubmed.ncbi.nlm.nih.gov/23518244/>.
 61. Zhang Y, Huang X, Duan B, Wu L, Li S, Yuan X. Preparation of electrospun chitosan/poly(vinyl alcohol) membranes. *Colloid Polym Sci*. 2007;285:855–63. Available from: <https://doi.org/10.1007/s00396-006-1630-4>.

Publisher's Note Springer Nature remains neutral with regard to jurisdictional claims in published maps and institutional affiliations.

Springer Nature or its licensor holds exclusive rights to this article under a publishing agreement with the author(s) or other rightsholder(s); author self-archiving of the accepted manuscript version of this article is solely governed by the terms of such publishing agreement and applicable law.